Радиофизика и радиоастрономия, 2011, т. 16, №4, с. 424-432

Multi-Look Radiometric Correction of SAR Images

O. O. Bezvesilniy, I. M. Gorovyi, V. V. Vynogradov, and D. M. Vavriv

Institute of Radio Astronomy of the National Academy of Sciences of Ukraine,
4, Chervonopraporna St., Kharkiv, 61002, Ukraine
E-mail: vavriv@rian.kharkov.ua

Received August 25, 2011

Deviations of the aircraft trajectory and instabilities of the aircraft orientation lead to non-uniform illumination of the ground by the antenna beam and, as a result, to radiometric errors in radar images obtained with airborne synthetic aperture radars (SAR). The clutter-lock technique is commonly used to avoid the radiometric errors. However, this approach leads to strong geometric distortions in SAR images in the case of fast and significant instabilities of antenna orientation. Here we propose a multi-look radiometric correction technique which can be used instead of the clutter-lock. The proposed approach has been tested by using a Ku-band airborne SAR system installed onboard a light-weight aircraft.

Keywords: synthetic aperture radar (SAR), airborne SAR, radiometric errors, radiometric correction, multi-look processing

1. Introduction

Synthetic aperture radars (SAR) are capable of obtaining high-resolution radar images of ground surfaces by using a physically small antenna [1]. The radar is mounted onboard a moving platform such as an aircraft or a satellite. Due to the platform motion, the radar transmits and receives radar pulses at different positions on the trajectory. By coherent processing of the collected radar data, a synthetic aperture with a very narrow beam is formed thus providing the high azimuth (cross-range) resolution. The high range resolution is achieved by using a common pulse compression technique, for example, by transmitting pulses with linear frequency modulation. The direction of the synthetic aperture beam (the synthetic beam) is fully controlled by the SAR data processing algorithm. Usually, the synthetic beam is formed to be in the elevation plane of the real antenna beam. In other words, the synthetic beam is pointed at the central line of the ground spot illuminated by the real antenna. If the real antenna beam is wide enough, then several independent synthetic beams can be built within the main lobe of the real antenna pattern. This technique is known as multi-look processing [1]. Each synthetic beam forms an independent radar image of the same ground scene called "SAR look". The non-coherent averaging of the SAR looks into one multi-look SAR image is used to suppress speckle noise.

Difficulties in data processing for airborne SAR systems come from the platform motion errors [2]. Most of SAR processing algorithms imply the straight-line aircraft motion with constant altitude, velocity and orientation. Deviations of the aircraft trajectory from a straight line and instabilities of the aircraft orientation, if not being properly compensated, lead to defocusing of SAR images as well as to geometric distortions and radiometric (brightness) errors in SAR images.

Assume that the problem of compensation of phase errors and range migration errors caused by trajectory deviations is solved. We expect that the SAR processing algorithm is capable of producing well-focused SAR images based on the real flight trajectory measured by the SAR navigation system. In this paper, we will consider the problem of correction of radiometric errors which arise in SAR images because of instabilities of the real antenna beam orientation or, in other words, because of non-uniform illumination of the ground scene by the real antenna beam.

ISSN 1027-9636

The problem of radiometric errors is illustrated in Figs. 1(a) and 1(b). Without orientation errors, the synthetic beam of the central look is directed to the center of the real antenna beam, and all SAR look beams are within the main lobe of the real antenna pattern, as shown in Fig. 1(a). Antenna orientation errors lead to the case when some of the SAR beams are directed outside the real antenna beam to non-illuminated ground areas, as shown in Fig. 1(b), resulting in radiometric errors.

The clutter-lock technique [3] is usually used to avoid radiometric errors in SAR images. Following this technique, the synthetic beams are built adaptively to be directed according to the variations of the real antenna beam orientation as shown in Fig. 1(c). In order to do this, the mean Doppler frequency (the Doppler centroid), which is used to set the synthetic beam direction, is estimated from the received radar data. As a result, the Doppler frequency of the matched filter of the synthetic beam is locked to the Doppler frequency to the clutter signal, and the direction of the synthetic beam is locked to the direction of the real antenna beam.

However, the synthetic beam orientation variations due to the clutter-lock naturally lead to geometric distortions in SAR images. The problem of geometric distortions is vital for SAR systems installed onboard light-weight aircrafts because of rough motion of such platforms [4]. The clutter lock technique is effective if the antenna beam orientation variations are slow in time. In this case, the geometric distortions can be corrected by resampling of the obtained SAR images to the correct rectangular grid on the ground plane. If orientation instabilities are fast and significant, the clutter-lock leads to strong geometric distortions in SAR images which cannot be easily corrected by resampling.

In this paper, we propose a multi-look radiometric correction technique which can be used instead of the clutter-lock. The idea of the approach is to form an extended number of looks to cover directions beyond the main lobe of the real antenna pattern as illustrated in Fig. 1(d). In such an approach, some of the SAR look beams are always presented within the real antenna beam despite of orientation errors. Now we describe how to combine these extended SAR looks to produce the multi-look SAR image without radiometric errors. The proposed method of a radiometric error correction does not require accurate measurements of the real antenna beam orientation variations. Suffice it to know the average antenna beam orientation for the whole data frame used to produce a SAR image with the accuracy to half the antenna beam width.

The proposed approach has been successfully tested by using a Ku-band airborne SAR system [5] developed and manufactured at the Institute of Radio Astronomy of the National Academy of Sciences of Ukraine. Preliminary results have been presented at conferences [6, 7]. In this paper, the method is described in details.

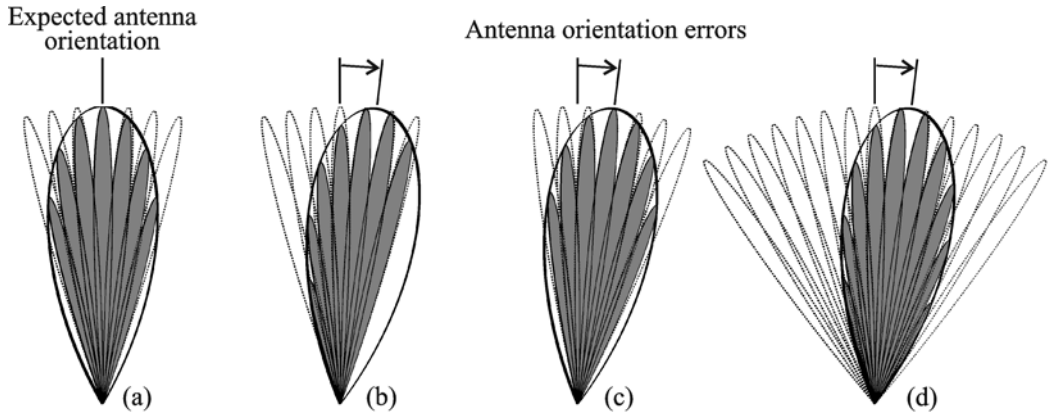

Fig. 1. *Multi-look processing without antenna orientation errors (a) and with orientation errors: without clutter-lock (b), with clutter-lock (c), with extended number of looks (d)*

2. Mathematical Model of Radiometric Errors

Let us denote the error-free SAR image to be reconstructed as $I(x, y)$, where (x, y) are the ground coordinates of the image pixels. This image is not corrupted by speckle noise and not distorted by radiometric errors. The obtained SAR look images $I(n_L, x, y)$ (n_L being the index of the SAR looks) are corrupted by speckle noise $S(n_L, x, y)$ and distorted by radiometric errors $0 < R(n_L, x, y) \le 1$ so that

$$I(n_L, x, y) = I(x, y)S(n_L, x, y)R(n_L, x, y). \quad (1)$$

The speckle noise in a single-look SAR image is a multiplicative noise [1] with the exponential probability density function with the mean and variance, correspondingly,

$$\mu\{S(n_L, x, y)\} = 1, \qquad \sigma\{S(n_L, x, y)\} = 1. \quad (2)$$

The speckle noise is uncorrelated for all SAR looks as indicated by the SAR look index n_L.

The radiometric errors caused by instabilities of antenna orientation are the low-frequency multiplicative errors. The highest spatial frequencies of the radiometric error function $R(n_L, x, y)$ typically correspond to the spatial scale of about half the width of the real antenna footprint in azimuth direction. Similar to the speckle noise, the radiometric errors are different for different SAR looks.

In order to compensate the radiometric errors we should measure them first. For this purpose we use a low-pass filter **F** to measure the local brightness of the SAR images. This filter is designed to pass the radiometric errors,

$$\mathbf{F}\{R(n_L, x, y)\} \approx R(n_L, x, y), \quad (3)$$

and at the same time, to suppress the speckle noise (2) to some extent:

$$\mathbf{F}\{S(n_L, x, y)\} \approx 1. \quad (4)$$

According to assumptions (3) and (4), the application of this filter to the SAR look image (1) gives approximately:

$$I_{LF}(n_L, x, y) = \mathbf{F}\{I(n_L, x, y)\} \approx I_{LF}(x, y)R(n_L, x, y). \quad (5)$$

Here $I_{LF}(x, y)$ is the low-frequency component of the error-free SAR image to be reconstructed. The low-frequency components of the SAR looks $I_{LF}(n_L, x, y)$ (5) contain information about the radiometric errors and are almost not corrupted by speckle noise. These images can be used to compare radiometric errors on different SAR looks and, though such comparison, to estimate and compensate the radiometric errors as described in the next section.

3. Multi-Look Radiometric Correction

3.1. Idea of the Method

The idea of radiometric correction by multi-look processing with the extended number of looks is based on the fact that the synthetic beam of one of many looks is pointed very close to the center of the real antenna beam. This look demonstrates the maximum power (brightness) among all looks, and this power is not distorted by radiometric errors. The mathematical description is as follows.

For every point of the scene we may find the brightest pixel among all SAR looks:

$$I_{LF}^{max}(x, y) = \max_{n_L = 1, \ldots, N_L^{ext}} \{I_{LF}(n_L, x, y)\}. \quad (6)$$

By substituting (5) into (6) we obtain

$$I_{LF}^{max}(x, y) \approx I_{LF}(x, y) \max_{n_L = 1, \ldots, N_L^{ext}} \{R(n_L, x, y)\}. \quad (7)$$

These brightness values are obtained with the synthetic beams that are directed very close to the center of the real beam. Therefore they are not distorted by the radiometric errors:

$$\max_{n_L = 1, \ldots, N_L^{ext}} \{R(n_L, x, y)\} \approx 1. \quad (8)$$

This means that the image $I_{LF}^{max}(x, y)$ (7) gives the estimate of the low-frequency component of the error-free SAR image to be reconstructed:

$$I_{LF}^{max}(x, y) \approx I_{LF}(x, y). \qquad (9)$$

This image can be used as the reference to estimate radiometric error functions for all SAR looks. From (5) and (9) we obtain

$$R(n_L, x, y) \approx \frac{I_{LF}(n_L, x, y)}{I_{LF}^{max}(x, y)}. \qquad (10)$$

By using the estimated radiometric error functions we may correct radiometric errors for all SAR looks before combining them into the multi-look SAR image.

3.2. Implementation of the Method

Let us denote the number of looks to be summed up into a multi-look image as N_L^{pro}. This number of looks should be slightly less than that within the real antenna beam N_L since the orientation instabilities may corrupt the side looks considerably. By using the low-pass filter we should select the brightest (best-illuminated) parts of the scene among all extended SAR looks with the indexes $n_L = 1, ..., N_L^{ext}$ and compose only N_L^{pro} SAR looks (called the composite looks) for further processing. It is convenient to build the following sequence of pairs of the composite looks and their low-frequency components:

$$\left\{I^{pro}(n_L^{pro}, x, y), I_{LF}^{pro}(n_L^{pro}, x, y)\right\},$$

$$n_L^{pro} = 1, ..., N_L^{pro}.$$

This sequence is kept in the ascending order with respect to the brightness:

$$I_{LF}^{pro}(n_L^{pro}, x, y) \le I_{LF}^{pro}(n_L^{pro} + 1, x, y).$$

After processing of all the extended SAR looks, the brightest composite look is the one with the index $n_L^{pro} = N_L^{pro}$. This look gives the estimate (9) of the low-frequency component of the error-free SAR image to be reconstructed.

If the number of looks N_L^{pro} is sufficiently large (e.g. greater than 9), we may improve the estimate (9) by averaging several brightest composite looks (e.g. 3 looks) to suppress the residual speckle noise which have leaked though the low-pass filter:

$$I_{LF}^{max}(x, y) = \frac{1}{3}\sum_{n=1}^{3} I_{LF}^{pro}(N_L^{pro} - n + 1, x, y).$$

The radiometric errors are corrected according to (10) as follows:

$$I_{RC}(n_L^{pro}, x, y) = I^{pro}(n_L^{pro}, x, y)\frac{I_{LF}^{max}(x, y)}{I_{LF}^{pro}(n_L^{pro}, x, y)}.$$

Finally, applying the above radiometric correction, we may build the multi-look SAR image as

$$I_{RC}^{pro}(x, y) = \frac{1}{N_L^{pro}}\sum_{n_{pro}=1}^{N_L^{pro}} I_{RC}^{pro}(n_L^{pro}, x, y). \qquad (11)$$

The main steps of the described algorithm are shown in Fig. 2.

3.3. Some Practical Considerations

We may use the Doppler centroid values estimated from the backscattered radar signal to prevent the synthesis of those SAR look beams which are obviously directed beyond the real antenna beam at the moment. This allows to reduce the computation burden. It is especially important when the variations of the real antenna beam orientation are larger than the antenna beam width, and we have to increase the number of the SAR looks considerably, although just a few of the extended SAR looks are illuminated simultaneously.

To improve the signal-to-noise ratio in the final multi-look SAR image, we should not sum up those SAR looks which are illuminated less than, for example, –10 dB with respect to the maximum illumination. Such poorly-illuminated SAR looks may introduce significant additional receiver noise to the final image. Actually, this threshold limits the possible number N_L^{pro} of the composite SAR looks.

The low-frequency components of SAR look images $I_{LF}(n_L, x, y)$ (5) can be obtained by using

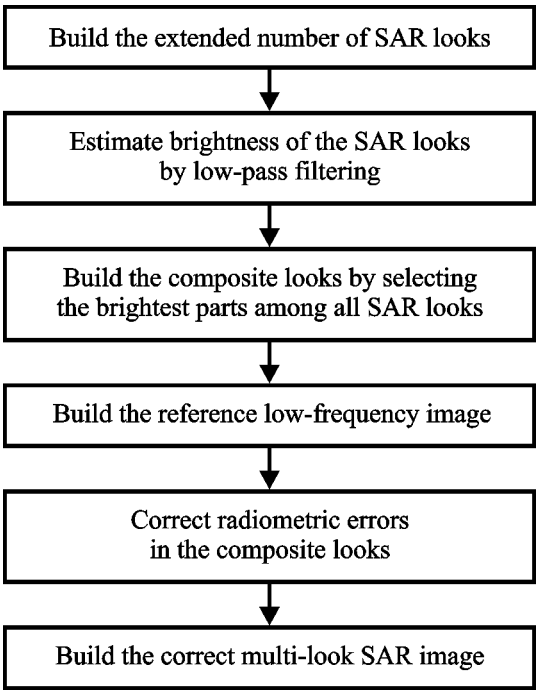

Fig. 2. *Main steps of the multi-look radiometric correction algorithm*

a simple smoothing filter, but excluding from averaging all bright points representing artificial objects. The radar cross section of artificial targets may demonstrate significant variations from one look to another hampering the correct choice of the best illuminated looks.

If the navigation system is capable of measuring accurately the fast variations of the real antenna beam orientation, and if we know the real antenna pattern, then we may calculate the radiometric error functions (10) directly from the relative orientation of the synthetic beam and the real antenna beam. This approach is more rigorous and accurate than the above-described empirical one with the image brightness estimation. Nevertheless, with this approach we still have to build the extended number of SAR looks, select the best parts of SAR images among all looks and form the composite looks for multi-look processing (11).

4. Experimental Results

The proposed method of a multi-look radiometric correction has been tested experimentally by using an airborne SAR system [5] installed onboard an Antonov AN-2 aircraft. Characteristics of the SAR system are listed in Table 1. The SAR system operates at the wavelength around 2 cm. The real antenna beam width is about 1° in azimuth and 40° in elevation. The slant range resolution is 3 m. For the same azimuth resolution of 3 m, SAR images can be built of 9 half-overlapping SAR looks under stable flight conditions.

Table 1. *RIAN-SAR-Ku system characteristics*

Transmitter	
Transmitter type	Traveling-wave tube power amplifier
Operating frequency	Ku-band
Transmitted peak power	100 W
Pulse repetition frequency (PRF)	5 – 20 kHz
Pulse compression technique	Binary phase codding (M-sequences)
Pulse bandwidth	50 MHz
Pulse duration	5 μs
Receiver	
Receiver bandwidth	100 MHz
Receiver noise figure	2.5 dB
ADC sampling frequency	100 MHz
ADC capacity	12 bit
Range sampling interval	1.5 m
Number of range gates	1024
Antenna	
Antenna type	Slotted-waveguide
Antenna beam width in azimuth / elevation	1°/40°
SAR Platform	
Aircraft flight velocity	30 – 80 m/s
Aircraft flight altitude	1000 – 5000 m
Aircrafts used	Antonov AN-2
SAR images	
Azimuth resolution	3 m
Range resolution	3 m
Range swath width	1536 m
Raw data recording	Range-compressed, 7-times decimated down from the PRF

Light-weight aircraft platforms – such as the AN-2 aircraft – suffer from significant trajectory deviations and orientation instabilities. The influence of motion errors is illustrated in Fig. 3, where you can see the coordinate grid in the radar coordinates "slant range – azimuth" projected into the ground plane. The horizontal curves are the curves of the constant slant range from the aircraft. They are curved because of deviations of the trajectory from the straight line. The vertical lines are the central lines of the antenna footprint (the Doppler centroid lines) for the consequent aircraft positions along the trajectory. As is seen, these central lines are non-equidistant and non-parallel because of variations of the antenna orientation.

If the clutter lock technique is applied, then the ground scene is sampled on the above-described radar coordinate grid, which is non-uniform with respect to the ground coordinate system. As a result, geometric distortions will appear in the SAR image as illustrated in Fig. 4. The geometric errors in this single-look SAR image built by using the clutter lock are evidently represented by the curved forest shelter belts between the fields in the top-left corner of the image and the curved road in the bottom-right corner of the image. The size of the scene in the SAR images is about 1.5 km in range (the vertical bottom-top direction) and about 2 km in azimuth (the horizontal left-right direction). The resolution in range and in azimuth is 3 m.

If we do not use the clutter-lock and if we do build the multi-look image as usual by using 9 central SAR looks, we will observe severe radiometric errors in the SAR image as shown in Fig. 5. Note, however, that the above-described geometric errors have disappeared from this SAR image.

The SAR image in Fig. 6 was built without the clutter-lock by simple averaging of all the extended SAR looks. The image demonstrates good geometric accuracy. You may compare now the top-right corners of the images in Figs. 4 and 6. You can see how the antenna beam movement "forward-backward-forward" distorts the shape of the forest area in Fig. 4 as compared to its correct shape in Fig. 6.

The radiometric errors are still present in the SAR image in Fig. 6. You can see dark and light strips in the image caused by non-uniform illumination of the scene. The dark areas were illuminated for shorter time, the SAR image was present only on a few SAR looks, the real antenna footprint quickly moved to the neighbor areas of the scene. The light areas were illuminated for longer

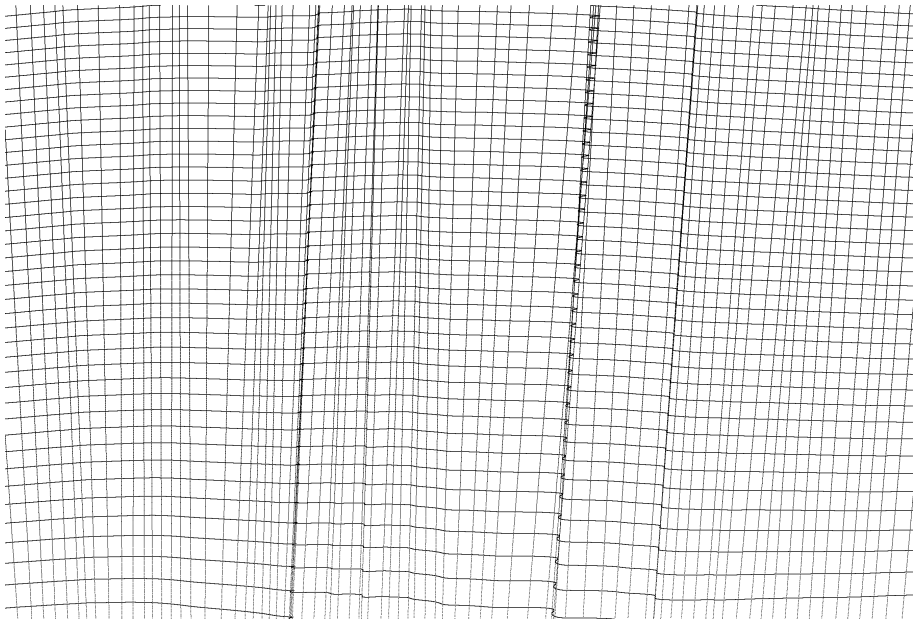

Fig. 3. *Trajectory deviations and orientation instabilities illustrated by the coordinate grid in the radar coordinates "slant range – azimuth" on the ground plane*

Fig. 4. *Geometric distortions in a single-look SAR image built by using the clutter lock*

Fig. 5. *Radiometric errors in the SAR image built without the clutter lock by simple averaging of 9 central looks*

time, the SAR image was present on many SAR looks.

The SAR image shown in Fig. 7 was built without clutter lock by using the proposed method of multi-look radiometric correction with the extended number of looks. The image was formed of 5 composite SAR looks. One can see that the radiometric errors have been corrected.

The proposed method of multi-look radiometric correction has been successfully applied in conjunction with the the two SAR processing algorithms: 1) the algorithm with the built-in geo-

Fig. 6. *Radiometric errors in the SAR image built without the clutter lock by simple averaging of all extended SAR looks*

Fig. 7. *Multi-look SAR image formed of 5 composite SAR looks by using the proposed radiometric correction*

metric correction [6, 8], and 2) the well-known range-Doppler algorithm [7]. It will be observed here that these SAR processing algorithms cannot be combined with the clutter-lock technique.

5. Conclusions

The proposed method of multi-look radiometric correction is an effective alternative to the clutter-lock technique. The method can be used with the

SAR processing algorithms that cannot be combined with the clutter-lock. The proposed method also allows correcting the radiometric errors in SAR images if the accurate orientation of antenna is unknown. The obtained experimental results have demonstrated that the method is capable of producing multi-look SAR images without geometric and radiometric errors under unstable flight conditions.

References

1. C. J. Oliver and S. Quegan, *Understanding Synthetic Aperture Radar Images*. Boston, London: Artech House, 1998, 480 p.
2. S. Buckreuss, "Motion errors in an airborne synthetic aperture radar system", *European Trans. on Telecommunications*, vol. 2, no. 6, pp. 655-664, 1991.
3. S. N. Madsen, "Estimating the Doppler centroid of SAR data", *IEEE Trans. Aerosp. Electron. Syst.*, vol. 25, pp. 134-140, Mar. 1989.
4. D. Blacknell, A. Freeman, S. Quegan, I. A. Ward, I. P. Finley, C. J. Oliver, R. G. White, and J.W. Wood , "Geometric accuracy in airborne SAR images", *IEEE Trans. Aerosp. Electron. Syst.*, vol. 25, no. 2, pp. 241-258, 1989.
5. D. M. Vavriv, V. V. Vinogradov, V. A. Volkov, R. V. Kozhyn, O. O. Bezvesilniy, S. V. Alekseenkov, A. V. Shevchenko, A. A. Belikov, M. P. Vasilevskiy, and D. I. Zaikin, "Cost-effective airborne SAR", *Radiofizika i radioastronomia*, vol. 11, no. 3, pp. 276-297, 2006.
6. O. O. Bezvesilniy, I. M. Gorovyi, V. V. Vinogradov, and D. M. Vavriv, "Correction of radiometric errors by multi-look processing with extended number of looks", in *Proc. of the 11th Int. Radar Symp. IRS* 2010 (Vilnius, Lithuania), vol. 1, 2010, pp. 26-29.
7. O. O. Bezvesilniy, I. M. Gorovyi, V. V. Vynogradov, and D. M. Vavriv, "Range-Doppler algorithm with extended number of looks", in *Proc. of the 3rd Int. Microwaves, Radar and Remote Sensing Symp. MRRS* 2011 (Kyiv, Ukraine), 2011, pp. 203-206.
8. O. O. Bezvesilniy, I. M. Gorovyi, S. V. Sosnytskiy, V. V. Vinogradov, and D. M. Vavriv, "SAR processing algorithm with built-in geometric correction", *Radiofizika i radioastronomia*, vol. 16, no. 1, pp. 98-108, 2011.

Многовзглядовая радиометрическая коррекция РСА-изображений

А. А. Безвесильный, Е. Н. Горовой, В. В. Виноградов, Д. М. Ваврив

Отклонения траектории самолета и нестабильности ориентации самолета приводят к неравномерной подсветке земной поверхности лучом антенны и в результате к радиометрическим ошибкам на радиолокационных изображениях, полученных с помощью самолетных радиолокаторов с синтезированной апертурой (РСА). Чтобы избежать радиометрических ошибок, обычно применяется техника слежения за сигналом от местности. Однако такой подход приводит к значительным геометрическим искажениям на РСА-изображениях в случае быстрых и значительных нестабильностей ориентации антенны. В этой статье мы предложили технику многовзглядовой радиометрической коррекции, которую можно использовать вместо слежения за сигналом от местности. Предложенный подход был испытан с помощью самолетного РСА 2-сантиметрового диапазона длин волн, установленного на легком самолете.

Багатопоглядова радіометрична корекція РСА-зображень

О. О. Безвесільний, Є. М. Горовий, В. В. Виноградов, Д. М. Ваврів

Відхилення траєкторії літака та нестабільності орієнтації літака призводять до нерівномірного підсвічування земної поверхні променем антени і, як наслідок, до радіометричних помилок на радіолокаційних зображеннях, отриманих за допомогою літакових радіолокаторів з синтезованою апертурою (РСА). Аби уникнути радіометричних помилок, звичайно використовується техніка слідкування за сигналом від місцевості. Однак такий підхід призводить до значних геометричних спотворень РСА-зображень у випадку швидких та значних нестабільностей орієнтації антени. У цій статті ми пропонуємо техніку багатопоглядової радіометричної корекції, яку можна використовувати замість слідкування за сигналом від місцевості. Запропонований підхід був випробуваний за допомогою літакового РСА 2-сантиметрового діапазону довжин хвиль, встановленого на легкому літаку.